DSP-Controlled Power Electronic Interface for Fuel-Cell-Based Distributed Generation

Annamalai Kirubakaran, *Member, IEEE*, Shailendra Jain, *Member, IEEE*, and Rajesh Kumar Nema

***Abstract*—The private power producers are increasing rapidly to meet rising load demand in domestic, commercial, and industrial sectors. In this scenario, the distributed generation systems (DGs) play an important role over fossil fuel generation. Among different distributed generation technologies such as fuel cell, wind power, and solar; the fuel-cell-based distributed generation is becoming more popular due to its high efficiency, cleanliness, modularity, and cost effectiveness. The development of a suitable power electronic interface and control schemes, therefore, play vital role in regulating fuel-cell voltage, both under steady and transient conditions. This paper, therefore, presents a DSP-controlled single stage power electronic interface for fuel-cell-based generation intended for residential/grid connected applications. The presented scheme generates pulse width modulation (PWM) control signals using TMS320F2812 DSP controller interfaced with MATLAB/Simulink model. A comprehensive simulink based model of the scheme is evolved and discussed. The experimental results are presented for varying loads and transient conditions.**

***Index Terms*—Code composer studio, DSP, polymer electrolyte membrane (PEM) fuel cell, power quality, pulse width modulation (PWM) inverter.**

I. Introduction

In RECENT years, the issues of growing energy demand, rising public awareness for environmental protection and existing nature of fossil fuels, have resulted in much of the research work to be focused on renewable energy sources. Many private sectors invest huge money to cater their prime loads under severity of power cut and to feed their peak demand locally using conventional diesel generators. These conventional power sources are getting limited due to their inefficient and untidy operation. Alternatively, the private sectors and utilities are now concentrating on distributed generations (DG) based on renewable energy sources with accrued benefits on account of higher efficiency, improved power quality, reliability, and environmental friendly nature for stand-alone as well as grid connected applications [1].

Fig. 1 shows the deployment of different renewable, clean power sources at various places in a ring main system. The rating of DGs can range from a few kW up to 100 MW depending on different applications. However, one of the major safety issue in distributed generation is inadvertent islanding that needs to be handled carefully [2]–[4].

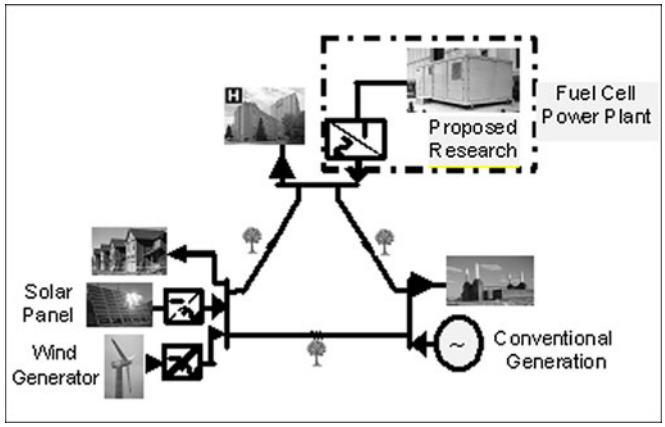

Fig. 1. Illustration of DG-based power generation.

The evolution of dispersed generation and microgrid may be accredited to two large power blackouts: 1) that occurred in 1999 at Southern Brazil and U.S., where more than 45 million people got isolated from the grid, and 2) in Northeastern and Midwestern United States, and Ontario, Canada, in 2003 [5]. These blackouts initiated both government officials and researchers to find out an alternate solution to provide uninterrupted power supply to the consumers.

Generally, the microgrid is defined as a cluster of loads with relatively small energy sources operating as single controllable network to supply consumer's power demands. One of the technical challenges with microgrid is the protection issue. It has to be isolated safely from the central grid during faults. Furthermore, it requires a large power capacity, control flexibility, and better quality of supply to meet local demands during islanding operation and utility grid connected operation [6]–[12]. It also requires high performance controllers for proper operation of the system in both grid connected and islanding modes. Many renewable distributed generations have intermittent power output and are interfaced using power converters. So, the fluctuating output may cause excessive voltage at some buses, overloading on some lines and power quality issues. To avoid complexity in control, the minimum communication between generations and loads are needed. This can be done by measuring required parameters from local grid or from the output of interfacing units. The real and reactive power sharing can be achieved by controlling independent variables, such as frequency and fundamental voltage magnitude. The different control techniques presented by various researchers are discussed in [9]–[11] to improve

Manuscript received June 4, 2010; revised October 23, 2010 and February 10, 2011; accepted March 19, 2011. Date of current version December 6, 2011. Recommended for publication by Associate Editor Josep M. Guerrero.

The authors are with the Department of Electrical Engineering, Maulana Azad National Institute of Technology, Bhopal 462 051, India (e-mail: a_kiruba81@rediffmail.com; sjain68@gmail.com; rk_nema@yahoo.com).

Color versions of one or more of the figures in this paper are available online at http://ieeexplore.ieee.org.

Digital Object Identifier 10.1109/TPEL.2011.2138162

the overall stability during load sharing with an autonomous microgrid system. A low voltage bipolar type dc microgrid for higher efficiency and higher power quality of supply is discussed in [12]. Available literature emphasizes on careful attention to the design, operation, safety, and control aspects of distributed generation before its deployment.

Among the different DG technologies, e.g., wind power, photovoltaic, micro turbine and fuel cells, the fuel-cell-based distributed generation is considered as one of the most promising technologies due to high operating efficiency (40–60%), cleanliness, modularity, reliability, and potential capability of providing both heat and power for combined cogeneration operation with efficiencies as high as 80% [13]. The wind turbine and photovoltaic power generation technologies are also being used to meet peak power demands. These technologies have obvious disadvantage that, they deliver power only when wind blows/sun shines and, hence, cannot be used as primary power source in grid connected operation. The wind power generation is although clean source of power, requires huge land for free air flow and contributes significantly to acoustic noise pollution. Because of its large size, the wind turbines take more installation time with relatively small addition to capacity. The solar photovoltaic generation on the other hand, when used for smaller capacity, need energy storage devices and when used for larger capacity, demands high investment and space as PV modules are less efficient. In contrast, a fuel-cell-based generation can provide continuous uninterrupted power supply to the consumers as long as input fuel is supplied. The grid interface of fuel cell is, therefore, considered as one of the probable area of promising research in microgrid environment.

Fuel cells are static energy conversion devices that convert chemical reaction of fuels directly into electrical energy and produces water and heat as its byproduct [14], [15]. It generates only dc power. The ideal output voltage of single cell is 1.2 V [16]. A number of cells are therefore to be connected in series so as to obtain a significant output voltage. These strings of series connected cells are again connected in parallel to increase available output power, thereby constituting a ''stack.'' Another serious problem with fuel cell is wide range of voltage variation under load conditions. A suitable power electronic interface is, therefore, necessary between given fuel cell stack and the load to achieve smooth voltage regulation, high efficiency, and galvanic isolation. However, the fuel cell current ripple reduction is a major issue for the fuel cell converter design, as it may cause thermal problem in fuel cell stacks and may also reduce its effective lifespan [17]–[19]. For safety aspects an electrical isolation is also important between fuel cell (FC) generation and stand-alone/grid connected loads. Fuel cell (FC) can be operated as a backup power source for grid-connected system to meet partial or full load demands.

The focus of the recent researches have been on the development of suitable low cost power electronic interface to address various inherent problems of fuel-cell-based generation, e.g., voltage regulation, power quality, and protection for stand-alone/grid connected applications.

Developments in digital control technology helped to enhance the power system stability via power flow control compared to analog controllers. Today, DSPs are considered as an efficient tool in real world applications for designing and implementing various control algorithms, especially in robotics, industrial automation, lighting, power supplies, and other control applications. The different control algorithms implemented for dc motor drive, dc-dc converter, power factor corrector, and multilevel inverter by program coding method are available in the literature [20]–[24]. MATLAB/Simulink Embedded Target mode of operation facilitates the implementation of DSP-based control in real time. A very limited literature is available on simple real time control [25]–[27], which is explored here.

Generally, the control algorithms can be developed by three methods, such as:

1) Programming source code using C/C++ or higher level language,
2) VisSim software with built-in DSP tools and,
3) MATLAB/Simulink model combined with Code Composer Studio (CCStudio) in RTW.

As for the above three methods are concerned, sampling and processing sine wave data in programming mode is difficult for the beginners and the use of VisSim software requires a high cost XDS560 JTAG emulator. However, the control algorithm developed in MATLAB/Simulink model can be easily implemented with the available library blocks in software package.

Looking into the possibility of huge potential in fuel cell based distributed generation, a laboratory proto-type of 1.2 kW capacity single stage DSP controlled power electronic interface is developed for residential applications. This paper presents a complete design and development of proposed single stage power electronic interface for 1.2 kW Nexa fuel-cell-based generation. The real time control in $dq0$ reference frame is developed using MATLAB/Simulink model interfaced with DSP TMS320F2812 to generate pulses for pulse width modulation (PWM) controlled converter. The complete description of the PWM pulse generation and associated control is presented. The effectiveness of the developed power electronic interface and the proposed control scheme is analyzed and validated through experimental results.

The paper is organized as follows. In Section II, a comprehensive review on power electronics interface and the significance of DSP controller are discussed. In Section III, complete design and hardware development of single stage power electronic interface is detailed out. Section IV brings forth complete description of DSP peripherals and PWM pulse generation method, and Section V presents the associated control scheme developed using F2812 eZdsp target. The experimental results are shown and discussed in Section VI with concluding remarks in Section VII.

II. Power Electronic Interface

The commercially available fuel cell generates voltage in the range of 25-50 V due to its higher production cost. The development of power electronic interface plays a vital role to convert fuel cell low output dc voltage into suitable form for residential/grid-connected applications. This can be achieved by using single stage dc/ac inverter topologies with a step up transformer or by a combination of dc-dc converter in series

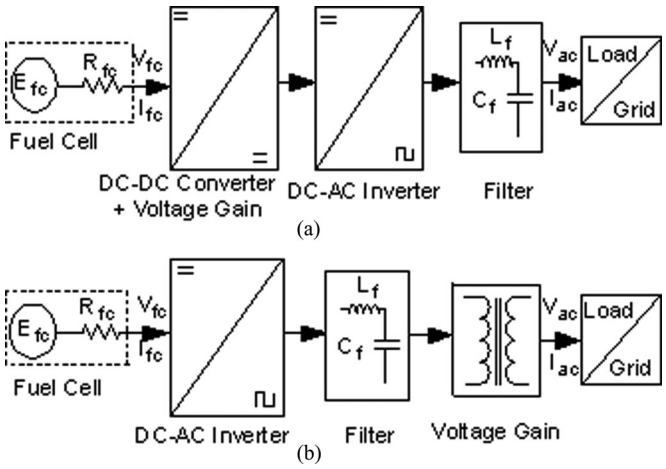

Fig. 2. Fuel-cell-based power supply system (a) Multi stage. (b) Single stage.

with dc/ac inverter forming multistage conversion, as shown in Fig. 2.

The selection of a suitable topology, switching frequency and controller decides the overall performance and cost of the system. Also, the efficiency of the system depends upon conduction and switching losses and cost of the system depends upon the total component count.

With the ideology of fuel-cell operation and requirement of low cost and efficient power interface, the different switch mode dc-dc converter topologies like conventional boost converter, push pull, half bridge, full bridge, etc., and dc-ac inverter topologies of 3-phase PWM inverter, Z source inverter, LLCC inverter, etc., have been proposed by various authors and are available in literature [28]–[46]. A comparison of different dc/dc converter and dc/ac inverter topologies based on their advantage and disadvantages are described in [17]. Generally, nonisolated dc/dc boost converter is preferred to step up dc voltage from one level to another due to its high efficiency and lower component count [29]. The isolated topologies, such as push pull, half bridge, and full bridge converters, can also be considered as candidate topologies for such applications. These topologies have some definite generalized benefits such as high boosting ratio and protective feature. The major problem with push pull converter is that half portion of the transformer cannot be symmetrically wound, resulting in transformer saturation under full load conditions. This makes its use restricted to low and medium power applications [30]–[32]. Alternatively, the half bridge converter with large transformation ratio can be used for high power applications, with matching dc link voltage. The full bridge converter although requires more number of switches yet it offers advantages in terms of reduced device current ratings, transformer turns ratio, and alleviated voltage and current stress across switching devices. The full bridge converter is thus suitable for high power applications with accrued benefits over half bridge converter [33]–[37]. The list is not yet complete and other dc/dc converter topologies such as current fed, series resonant H-bridge have also been developed for fuel cell applications and available in [38]–[44]. While in dc-ac inverter, a 3-phase PWM converter gives better performance, due to higher

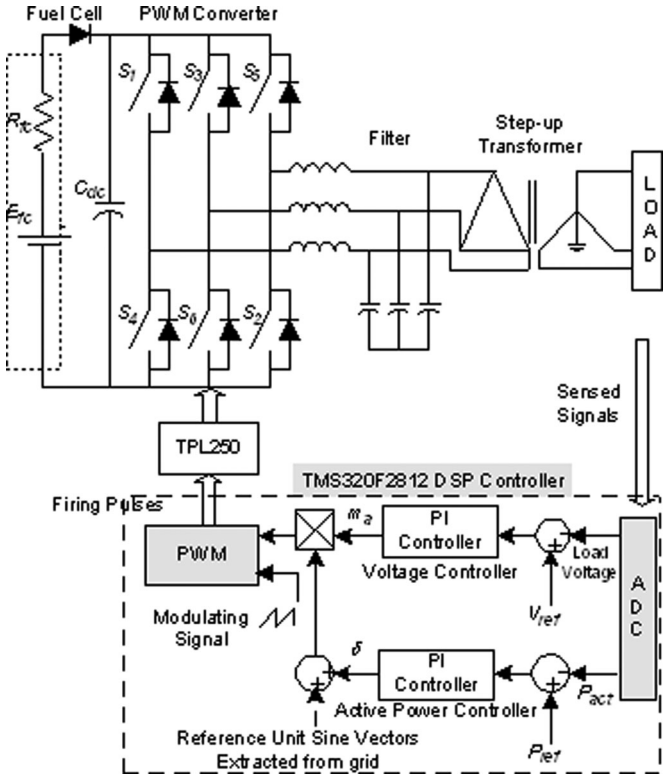

Fig. 3. Power circuit with closed loop control scheme.

efficiency, economic use of low voltage level MOSFET switches and simplicity in control. The Z source and LLCC inverter can be used if there is no electrical isolation required between fuel cell and load [45], [46].

In addition, the digital control has many advantages of programmability, low part count and reduced susceptibility to environmental concerns over analog control. The carrier frequency for the PWM scheme can also be changed simply through reprogramming. It also has the disadvantage that the width of the pulse is limited by the computation time of the DSP, since maximum pulse width is less than one sampling interval. This limitation results in lower output voltage amplitude than the supplied dc voltage. This problem can be rectified by proper selection of operating frequency of the digital signal processor. Therefore, in this work a DSP controlled single stage power electronic interface is developed for fuel cell based household/grid applications.

III. Proposed Power Electronic Interface

The single stage power electronic interface for fuel cell based power system consists of fuel cell stack, dc/ac inverter, LC filter, and step up transformer for stand-alone/grid connected applications, as shown in Fig. 3.

The complete control scheme is developed in $dq0$ reference frame to regulate the ac output voltage by controlling the modulation index (m_a) and the active power flow by adjusting the phase angle (δ) of the inverter voltage. The complete system design is as follows.

A. Polymer Electrolyte Membrane (PEM) Fuel Cell Model

Generally speaking, the characteristic of the fuel cell is decided by its thermodynamics and electrical efficiency of the system. The thermodynamic efficiency depends upon fuel processing, water management and temperature control of the system. The electrical efficiency on the other hand depends on various losses that take place in the fuel cell such as ohmic loss, activation loss and concentration loss. The steady state I-V characteristic curve is computed by using Tafel equation, as

$$V_{\rm fc} = V_{\rm open} - V_{\rm ohm} - V_{\rm act} - V_{\rm con} \tag{1}$$

where $V_{\rm fc}$ is output voltage of the fuel cell, $V_{\rm open}$ is the reversible open cell voltage, $V_{\rm ohm}$ is ohmic loss, $V_{\rm act}$ is activation loss and $V_{\rm con}$ is the concentration loss.

$V_{\rm open}$, $V_{\rm ohm}$, $V_{\rm act}$, and $V_{\rm con}$ for a PEM fuel cell can be computed with electrochemical modeling and using appropriate expressions as described in [47]. The ohmic loss is mainly due to resistance of nonideal electrodes and conduction of protons through its path. Under light loading conditions, the ohmic loss becomes less significant and the increase in output voltage is mainly due to activity of chemical reactions (time taken for warm up period). The losses due to the rate of reactions taking place on the surface of the electrodes are called activation losses. Activation loss results in reduced fuel cell efficiency during startup. A sudden increase in load may therefore cause damage to the stacks due to slow chemical reactions. The FC voltage droops significantly under heavy loading conditions because of the reduction of gas exchange efficiency. This region is generally called as concentration region and may be attributed to mass transport losses. In order to meet load demand under light and heavy loading conditions, the energy storage devices like batteries or capacitors are needed. The energy storage device not only supply auxiliaries at various stages but also improves slow transient response of the fuel cell [31], [35], [48]. This can also be done easily in micro grid system combined with one or other energy sources.

A Nexa 1.2 kW PEM fuel cell model is considered in this work. Practically measured I-V characteristics curve of the Nexa PEM fuel cell is shown in Fig. 4. For constant hydrogen input fuel supply, the fuel cell can be operated safely in linear range of voltages 26 V to 36 V and stack currents of 10 A to 45 A [49]. The linear portion is, therefore, considered for better voltage regulation and calculated using internal resistance only. The linearized output voltage due to its ohmic nature is given by

$$V_{\rm fc\_lin} = V_{o\_lin} - R_{\rm in\_lin} I_{\rm fc} \tag{2}$$

where $V_{\rm fc\_lin}$ is the linearized output voltage, $V_{o\text{-}\rm lin}$ is the linearized voltage without the load and $R_{\rm in\_lin}$ is the linearized internal resistance.

B. Power Circuit

A 2.4 Ω, 600 W resistor is connected in series with a 48 V battery so as to obtain the linear portion of I-V characteristics of a PEM fuel cell and 3-phase voltage source PWM inverter is used as single stage power electronic interface. A discrete 3-leg

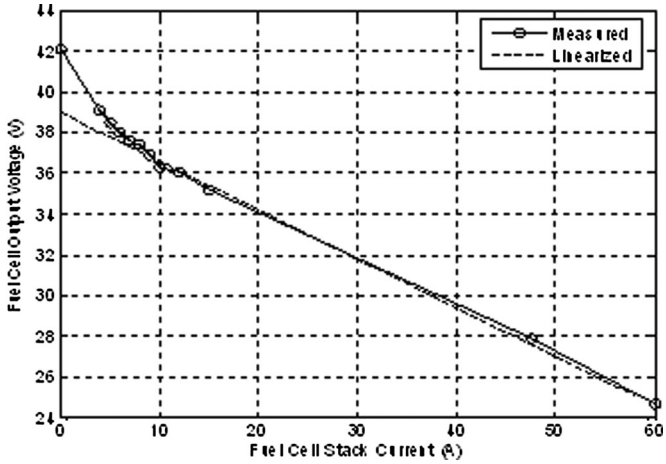

Fig. 4. Measured output characteristic of the Nexa.

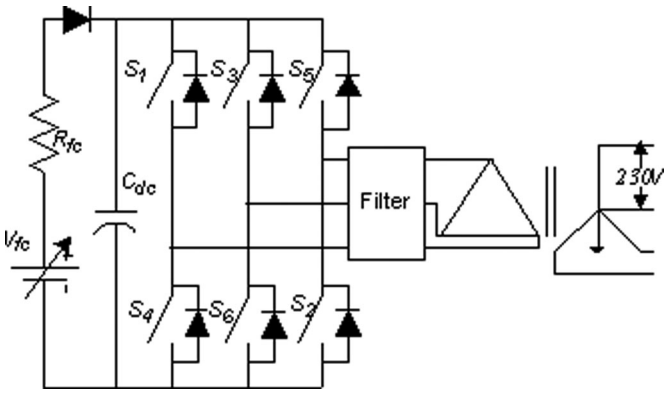

Fig. 5. Power circuit.

High power MOSFET IRF460 (21 Amps, 500 Volts) module is used to implement the 3-phase bridge inverter. The power circuit of PWM inverter consists of 6 MOSFET switches *(S_1 to S_6)* with integrated anti-parallel diodes *(D_1 to D_6),* as shown in Fig. 5. Suitably designed snubber circuits are connected across each device to limit the *dv*/*dt* and mounted on a suitable heat sink to ensure proper heat dissipation. To filter out harmonics in PWM inverter output, a suitably designed LC filter is used. The filtered voltage is stepped up from 14 V (LL) to 230 V (LN) with the use of 3-phase, 1.2 kVA, delta/star-connected transformer. The terminal voltage of inverter is controlled by comparing signals sensed from load side with the reference signal to generate firing pulses for switches S_1–S_6.

C. LC Filter Design

Any distributed generation scheme needs to confirm to power quality standards demanded by utility/consumer. It is, therefore, necessary to embed an output filter to eliminate harmonics injected by inverter and nonlinear loads present in the system. In this work, a switching frequency of 2 kHz is selected for PWM inverter operation. This renders a frequency modulation ratio "$mf = 40$," and lower order frequency component produced is of the order of $mf \pm 2$ [50] and above. These harmonics are effectively filtered out at the inverter terminal to improve

TABLE I
SELECTION OF TRANSFORMER TURN RATIO

V_{FC}	$I_{FC,max}$	$P_{FC,max}$	$V_{LL,P}$	$V_{LL,S}$	N_2/N_1	$I_{S,LN}$	$I_{P,LL}$	m_a
26V	45A	1170W	14.3V	400V	1:28	5.09A	47.24A	0.9

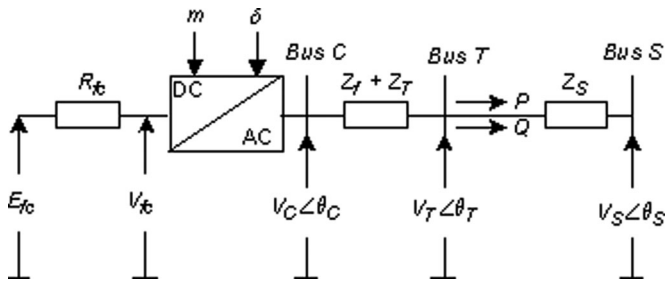

Fig. 6. Single line diagram of fuel-cell power plant.

quality of power. A cut-off frequency of 650 Hz is, therefore, considered, which is about 13 times greater than fundamental frequency and two times lower than switching frequency so as not to attenuate the fundamental component of 50 Hz frequency. To achieve better harmonic reduction in phase current and voltage, the values of filter input inductor *(L_f)* and capacitor *(C_f)* can be calculated by optimizing the filter parameters based on the following equation [51]:

$$f_c = \frac{1}{2\pi\sqrt{L_f C_f}}. \tag{3}$$

The calculated values for filter components come out to be 0.3 mH and 180 μF.

D. Transformer Design

The filtered output voltage is stepped up through a transformer to 230 V rms per phase for residential/grid connected loads. The calculated transformer parameters for primary line current, secondary phase current and turns ratio for the singe stage power electronic interface by assuming the worst case maximum loading of 1170 W (for 1200 W Nexa FC) are given in Table I.

E. Mathematical Modeling

A fuel-cell-based system is usually interfaced with ac grid at low/medium voltage level using a converter transformer. The single line diagram of fuel cell power plant (FCPP) representing 3-phase, symmetrical, balanced steady state system is shown in Fig. 6. The fuel cell is represented by a constant voltage source $E_{\rm fc}$ with internal resistance $R_{\rm fc}$ is connected to the SPWM inverter. Z_T and Z_f are impedances of transformer and filter inductor. The bus *T* is FCPP interface bus to the grid. The utility grid is represented by an infinite bus with constant voltage source (V_S, f_S) and short-circuit impedance Zs.

To study static and dynamic characteristics of the FCPP, S. Jain *et. al*. [52] have developed a mathematical model using *qd*0-reference frame. The model is developed in per unit (pu) system and is generalized to be used with systems of any rating.

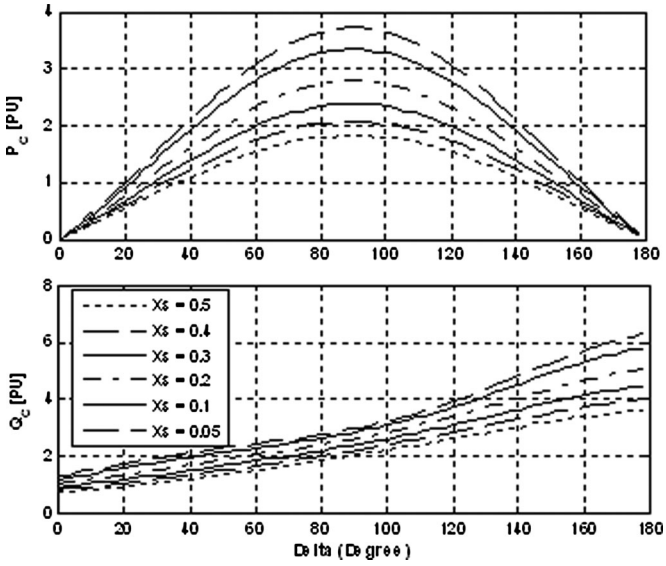

Fig. 7. Variation of active power and reactive power with respect to δ.

The derived expression for active, reactive power and voltage at the converter bus *C*, in terms of system variables such as fuel cell ($R_{\rm fc}, E_{\rm fc}$), converter ($m_a, \delta_{\rm CS}$), filter and transformer (Z_f, Z_T) and utility (V_S, Z_S) are as follows:

$$V_C = m_a E_{\rm fc} - \frac{m_a^2 R_{\rm fc}}{X} V_S \sin\delta_{\rm CS} \tag{4}$$

$$\begin{bmatrix} i_q \\ i_d \end{bmatrix} = \frac{1}{X}\begin{bmatrix} V_S \sin\delta_{\rm CS} \\ m_a E_{\rm fc} - V_S\left(\cos\delta_{\rm CS} + \dfrac{m_a^2 R_{\rm fc}}{X}\sin\delta_{\rm CS}\right) \end{bmatrix} \tag{5}$$

$$P_C = \frac{m_a E_{\rm fc} V_S \sin\delta_{\rm CS}}{X} + m_a^2 R_{\rm fc}\left(\frac{V_S \sin\delta_{\rm CS}}{X}\right)^2 \tag{6}$$

$$\begin{aligned} Q_C = {} & \frac{m_a^2 E_{\rm fc}^2}{X} + \frac{m_a^3 E_{\rm fc} R_{\rm fc} V_S \sin\delta_{\rm CS}}{X^2} \\ & - \frac{m_a R_{\rm fc} V_S \cos\delta_{\rm CS}}{X^2} \\ & + \frac{m_a^3 E_{\rm fc} R_{\rm fc} V_S \sin\delta_{\rm CS}}{X^2} \\ & + \frac{m_a^2 R_{\rm fc} V_S^2 \sin\delta_{\rm CS}\cos\delta_{\rm CS}}{X^2} \\ & - \frac{m_a^4 R_{\rm fc}^2 (V_S \sin\delta_{\rm CS})^2}{X^3} \end{aligned} \tag{7}$$

where m_a is the inverter modulation index, δ is the inverter angle, *X* is the system reactance, V_C is the converter voltage, I_q and I_d are the *dq*-axis currents and P_C, and Q_C are the active and reactive power supplied by the fuel cell.

From (4) to (7), the effect of power system and fuel cell parameters on power flow can be studied. Fig. 7 shows the

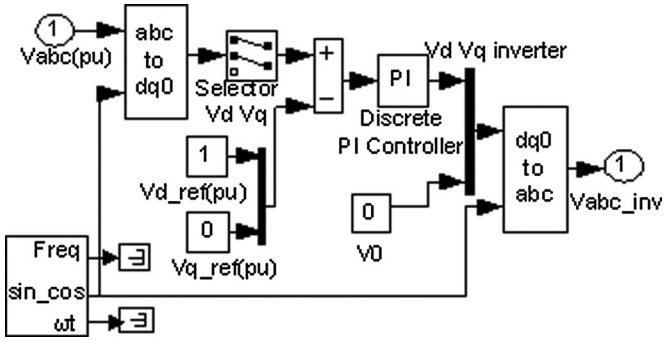

Fig. 8. Control scheme developed in MATLAB/Simulink.

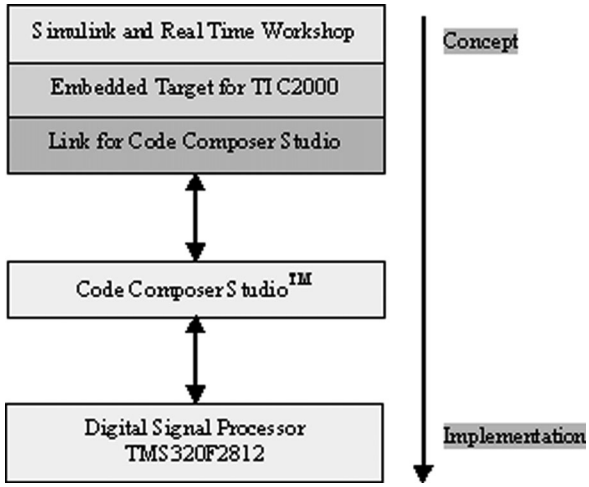

Fig. 9. The steps from the model to the implementation.

variation of power flow as a function of power angle ''δ'' keeping m_a constant for various values of system impedance. The maximum power transfer occurs at $\delta_{\rm CS} = 90^o$ and its value depends on system impedance as can be inferred from Fig. 7. This is similar to power angle characteristics of a system with two active ac sources. However, maximum power flow $P_{C\max}$ is a function of the parameters of both fuel cell and power system.

IV. Development of DSP Control

In this work, the main objective of using DSP controller is to generate PWM firing pulses for dc/ac inverter and to regulate magnitude of load voltages during load variations. The control scheme developed in *dq*0-reference frame in MATLAB/Simulink environment is implemented using TMS320F2812 DSP controller for real time applications as shown in Fig. 8. This section presents complete description of MATLAB/Simulink model interfacing with DSP in real-time workshop and PWM firing pulse generation methodology are presented. The use of DSP has, however, facilitated the implementation of proposed concept.

A. Overview of Digital Signal Processor

Implementation of high speed and complicated control schemes alongwith high sampling rates have led to a development of low cost digital signal processors. It was first developed by the Faculty of Engineering and Computer Science at the Institute of Robotics. In 1983, the Texas Instruments (TI) produced the first DSP TMS32010 with 16-bit operation. Progressively, a series of processors such as, C6000 DSPs, C5000 DSPs, OMAP Processors, and C2000 DSPs are made available with different features and various applications. The TMS320F2812 DSP controller is a 32-bit fixed point processor operating at 150 millions of instructions per second (MIPS), equipped with various control centric peripherals of analog to digital converters (ADC), two independent event managers (EVA & EVB), 12 PWM output ports, 56 individually programmable GPIO lines, built-in WATCHDOG & JTAG debug interface, various program/data memory, etc., [53]–[59].

In addition, a serial interface with 38.4 k baud rate is used to download the program into internal/ external memory. The TMS320F2812 DSP also supports C/C++ compiler; users familiar with the C language can easily develop their complicated control schemes using C/C++ apart from high-level language. But the complicated issue is synchronization between the sensed signals and generation of firing pulses.

B. C2000 Embedded Target

The overall process of code generation for MATLAB/Simulink model interface with CCStudio in real time workshop is shown in Fig. 9. Generally, Simulink Embedded Target TI C2000 is used to construct the closed loop system model using standard libraries available in MATLAB version R2007a. The Embedded Target of eZdsp 2812 block is added to Simulink model without any links, i.e., stand-alone mode operation and supports all futures of F2812 processor. This can also be implemented using other DSPs such as TMS320F2407 or C6000. Each DSP peripherals like ADC, DI, DO, CAN, PWM, QEP, and Read/Write Memory can be configured through graphical interface available in Simulink library. The acquisition of data from ADC is synchronized with PWM signal generation by proper scaling of IQ math and initializes necessary peripherals for required switching frequency. Since IQ math library allows user to start code development in floating point space. The code generated by real-time workshop for each of the blocks developed in MATLAB/Simulink is defined by Target Language Compiler (TLC) script in .tlc file. Finally, the developed model is interfaced with code composer studio to build the project [25], [54], [56].

C. Code Composer Studio

Code Composer Studio (CCStudio) is an integrated development environment (IDE) and provides an integrated platform for design, simulation, implementation and verification of embedded control systems on standard, and custom T2000 targets and other processors. Texas Instruments has various version of CCStudio v3.1, v3.3, and recently they have released v4. It includes a built-in editor, compiler, assembler, linker, and an automatic build process feature [57], [58]. In addition, built in graphical output facilities is also available. CCStudio

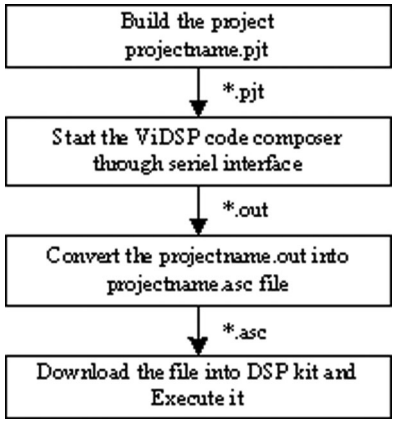

Fig. 10. CCStudio working procedure.

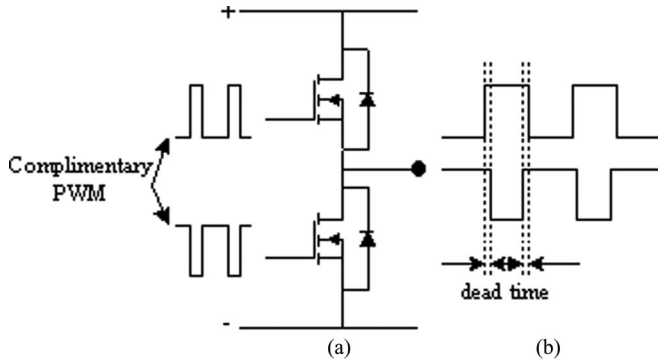

Fig. 11. (a) Complimentary PWM. (b) Dead time.

provides a single user interface taking users through each step of application development flow. The generated code by RTW is loaded to CCStudio and build process is carried out with the project title name attached to it automatically. The linker command .CMD is used to identify the memory location and directing the signals ''where to go,'' which results in .OUT file (projectname.out) at the linker output terminal. The projectname.out file is subsequently converted into projectname.asc by using ViDSP code composer. Finally, the projectname.asc file is downloaded to the DSP through serial port. The complete working procedure of CCStudio to build and executes the desired project is given in Fig. 10.

D. C2000 2812 DSP peripheral PWM Generation

The generation of the PWM algorithm requires following 2812 peripherals to sense voltage and the current signals, reference time, compare mechanism and digital outputs.

1) Analog to Digital Converters: The ADC module consists of a 12-bit, 16 channel ADC with two built-in sample-and-hold (S/H) circuits. The functions of the ADC module include 12-bit ADC core with fast conversion rate of 80 ns at 25-MHz ADC clock, 12.5 MIPS. The analog input signal is converted into equivalent digital value by using the following (8) [55]

$$\text{Digital Vaule} = 4095 * \frac{(\text{Input Analog Voltage} - \text{ADCLO})}{3} \tag{8}$$

where ADCLO is the ADC lowest operating voltage [ideally zero].

From (8) above, it is observed that ADC gives digital output from 0 to 4095 for changes in signal from 0 to maximum of 3 V. Therefore, one of the major constraints with ADC is that it can be operated only in specified region of 0 to 3 V, and as a result the DSP does not support any negative values, whereas the sine wave data type conversion requires processing of negative signal as well. The negative signal is taken care of by suitably shifting the amplitude of the negative signal with fixed dc voltage level using a positive clamping circuit. The 16 channel ADC has the ability to sample two ADCINxx sequentially, or simultaneous from one input in the range of ADCINA0-ADCIN07 and the second from ADCINB0-ADCINB7 to service event managers A and B [58]. They can also be operated as cascaded 16-channel module. The start of conversion is triggered by one of the following methods such as signal from software, EVA, EVB and external hardware. However, time for the start of conversion pulse has to be decided by width of the samples. To synchronize the ADC with the PWM pulses a hardware interrupt is used for effective control. For that, the ADC control and interrupt logic is implemented by using one of the four maskable interrupts like none, underflow interrupt, period interrupt and compare interrupt.

2) Event Manager Modules: The event manager modules are the main DSP blocks for PWM signal generation. The TMS320F2812 controller has two event managers A and B. Each module includes general purpose (GP) timers, capture units, quadrature encoder pulse (QEP) circuit and six independent pairs of PWM compare units that can be operated individually or in cascaded mode depending on the requirement [59]. In PWM block, module A displays three sets of *PWM*1/*PWM*2, *PWM*3/*PWM*4, *and PWM*5/*PWM*6 compare units and module B displays three sets of *PWM*7/*PWM*8, *PWM*9/*PWM*10, *and PWM*11/*PWM*12 compare units. The performance of the EVA and EVB module is controlled independently by two GP timers to provide a time-based operation for compare units and associated PWM circuits to generate the PWM outputs. The GP Timers 1 and 2 are controlled by event manager A, and GP Timers 3 and 4 are controlled by event manager B.

3) General Purpose Timers: Each GP timer has a 16 bit up-down counter *TxCNT*, a compare register *TxCMPR*, a period register *TxPR*, an individual control register *TxCON* for Read/Write operations, and a direct input *TDIRx* register is used for up/down counting operations. This GP timer counter is used to generate either asymmetric or symmetric carrier signals for required sampling frequency by using *TxCON*. The asymmetric and symmetric carrier waveforms are generated by continuous count-up mode and up-down mode of operation respectively. The compare register associated with each GP timer is used for PWM pulse generation. The pulse widths of the PWM outputs are determined by the values given in the compare register. During compare matches the PWM changes its state from 0 to 1 or from 1 to 0 and the count value also goes up or down depending on the nature of sign matches (+ or –). These logic output shows that the state of PWM pin either as active high or active low. The polarity of PWM outputs can be selected by enabling registers either active high and active low or forced high and forced low.

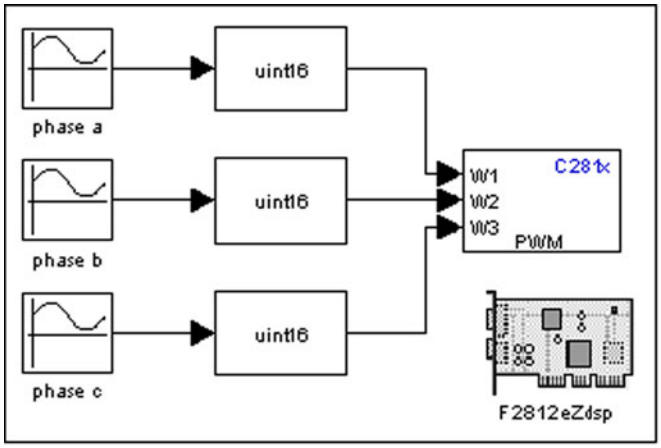

Fig. 12. Open loop control model.

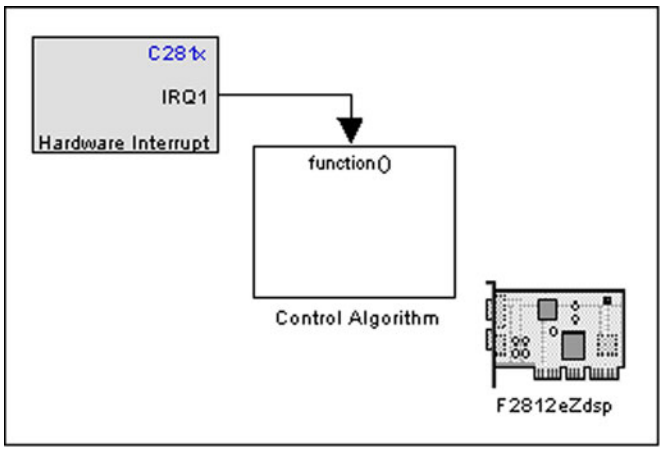

Fig. 13. Closed loop control model.

4) Introducing Delay: Generally speaking, the gate turn ON is faster than the turn OFF, in MOSFET switches. This may result in shoot through problems occurring across upper and lower switches of a same leg when operating at complementary PWM pulses, as shown in Fig. 11(a). This causes a high current to be drawn from the power supply, excessive heat production, and over stress across the switching devices and the power supply. Therefore, a dead time is introduced between the pulses by selecting the suitable values of dead band prescaler and dead band period given in the PWM block. Fig. 11(b) shows the complementary PWM with dead time.

5) Carrier Signal Generation: The carrier signal waveform period for a selected frequency is given by [60]:

$$f_{\mathrm{pwm}} = \frac{f_{\mathrm{HSPCLK}}}{(\mathrm{Waveform\ Period})} \cdot \frac{1}{2} \tag{9}$$

where

$$\mathrm{waveform\ period} = \frac{f_{HSPCLK}}{(2x f_s)} \tag{10}$$

where f_{HSPCLK} is the frequency of the high speed peripheral clock and f_s is the switching frequency. The term $\frac{1}{2}$ is used due to the symmetrical waveform. It is desired to get a 2 kHz

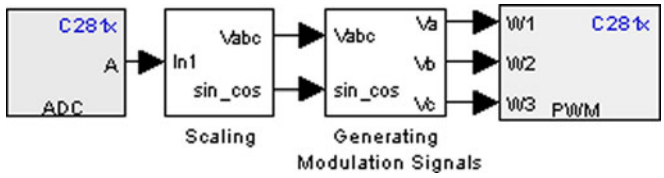

Fig. 14. Simulink model of control algorithm.

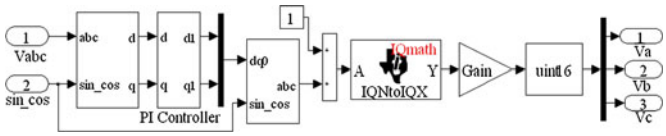

Fig. 15. Simulink model for generating modulation signals.

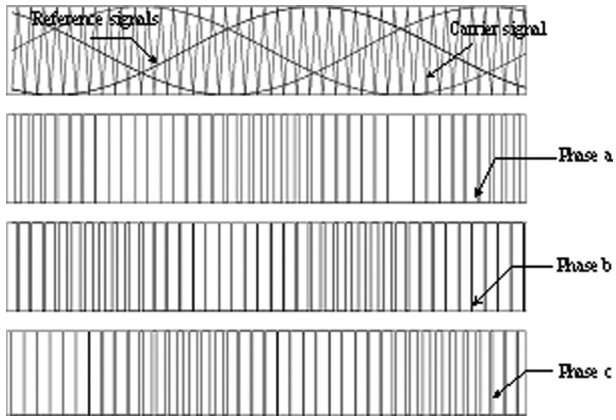

Fig. 16. PWM control waveforms.

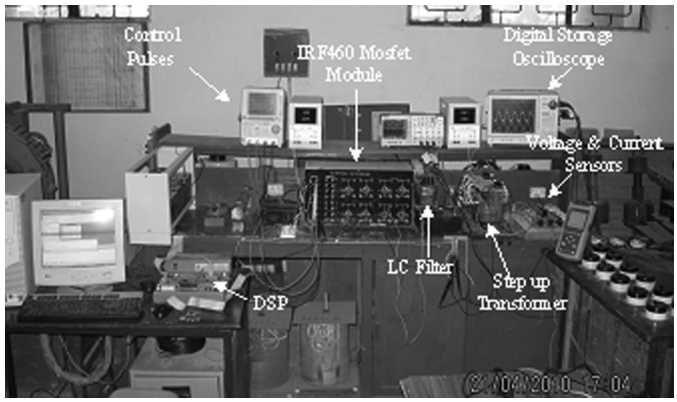

Fig. 17. Experimental setup.

carrier signal in symmetric form for 50 MHz of $\mathrm{f_{HSPCLK}}$, the calculated waveform period is

$$\mathrm{waveform\ period} = \frac{50\,\mathrm{MHz}}{(2 \times 2000)} = 12500.$$

The selection of $f_{\mathrm{HSPCLK}} = GP\,\mathrm{TImer} \times \mathrm{CLKIN} = 50\,\mathrm{MHz}$ value is obtained by adjusting the parameters of HISPCP [2-0] = 3, PLLCR [3-0] = 10, TICON [10-8] = 0, and TIPR = 12 500. However, any one of the following HISPCP values of 1, 2, 4, 6, 8, 10, 12, or 14 can be selected to adjust f_{HSPCLK} to the required frequency.

Table II
EXPERIMENTAL PARAMETERS

Parameters	Values
Power Rating	1200VA
V_{fc}	40V (no load)
R_{fc}	0.24 Ω
AC Filter	R_f= 0.5 Ω, L_f= 0.3 mH, C_f= 180μF (on each phase)
Step Up Transformer	14V/400V, 1.2 kVA, 50Hz, Delta/Star connection
MOSFET Switches	IRF460
Ron	0.27Ω
Device (V_f)	1V
Diode (V_{fd})	0.7V

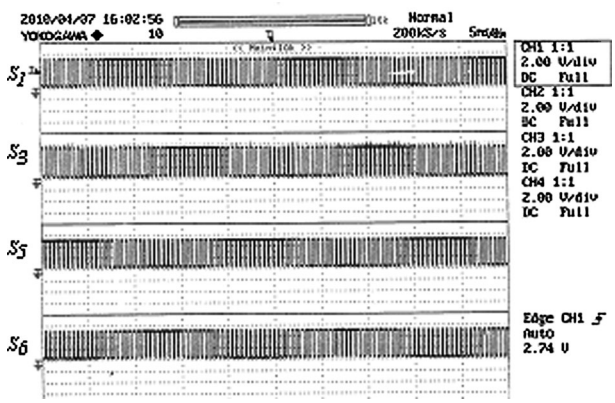

Fig. 18. Control pulse generated from PWM block in DSP.

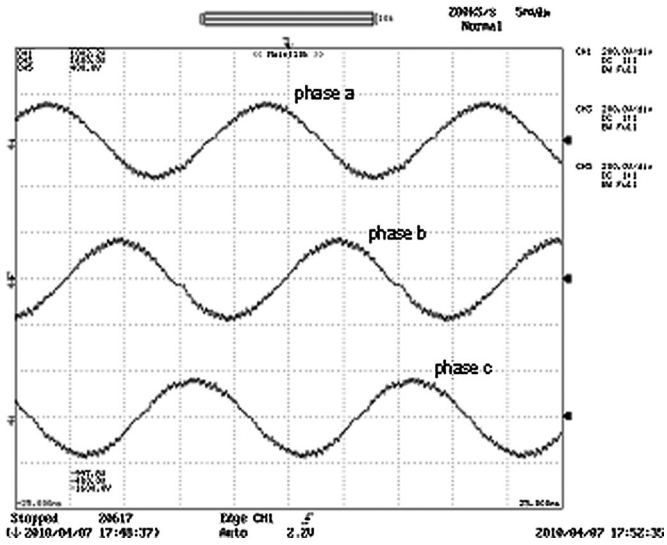

Fig. 19. Three phase output voltage waveform for 180 W resistive load.

V. CONTROL SCHEME

Fig. 12 shows the open loop control scheme developed in MATLAB/Simulink with F2812 eZdsp target in real time workshop. The amplitude of the calculated sine waveform can be varied from 0 to 6250 for corresponding changes in fixed modulation index from 0.5 to 1. It should be noted that the negative

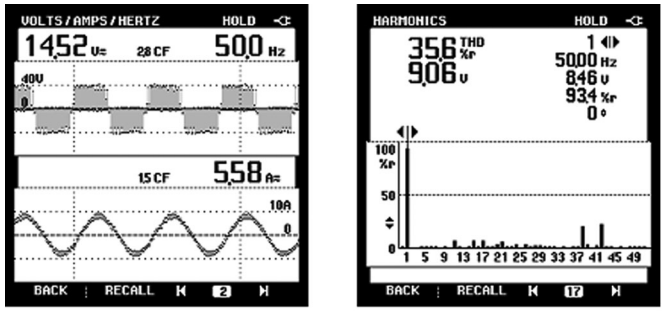

(a) (b)

Fig. 20. (a) Inverter output voltage and primary current of the transformer. (b) Frequency spectrum of inverter output voltage (for 180 W resistive load).

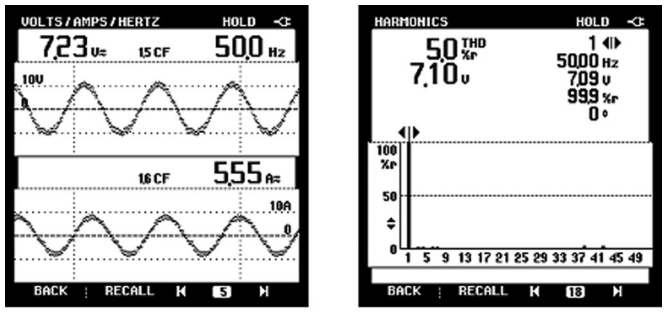

(a) (b)

Fig. 21. (a) Experimental results of filtered output voltage and primary current of the transformer. (b) Frequency spectrum of filtered output voltage (180 W resistive load).

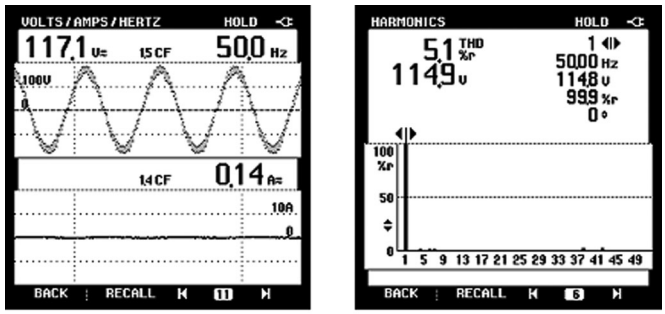

(a) (b)

Fig. 22. (a) Line to neutral ac output voltage, and (b) Frequency spectrum of filtered output voltage (180 W resistive load).

portion of the sine wave is biased to positive side with an offset value of 6250, since the analog to digital converter (ADC) accepts only positive values. The three phase signals are passed through *"unsigned integer* 16*"* to the PWM block to compare with the carrier signal waveform period of 12500 and to generate pulses.

In closed loop control scheme, the control algorithm is developed in *dq*0 reference frame with power circuit as shown in Fig. 13. The various blocks involved in MATLAB/Simulink to implement the closed loop control algorithm in real-time interface targeted with TMS320F2812 DSP controller are shown in Figs. 14 and 15.

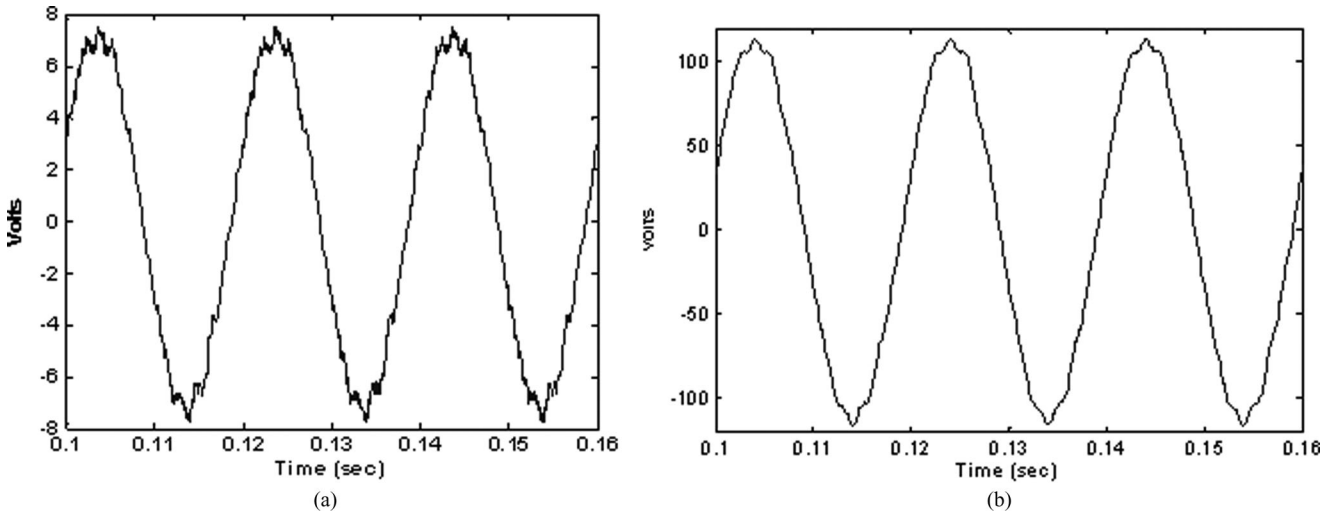

Fig. 23. (a) Simulation result of filtered output voltage. (b) Line to neutral ac output voltage.

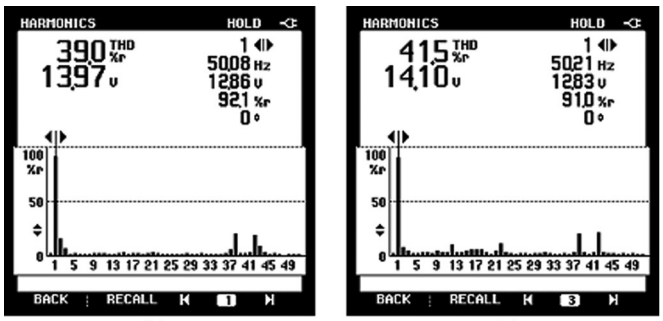

Fig. 24. Frequency spectrum of inverter output voltage for varying loads (a) 180 W (b) 300 W.

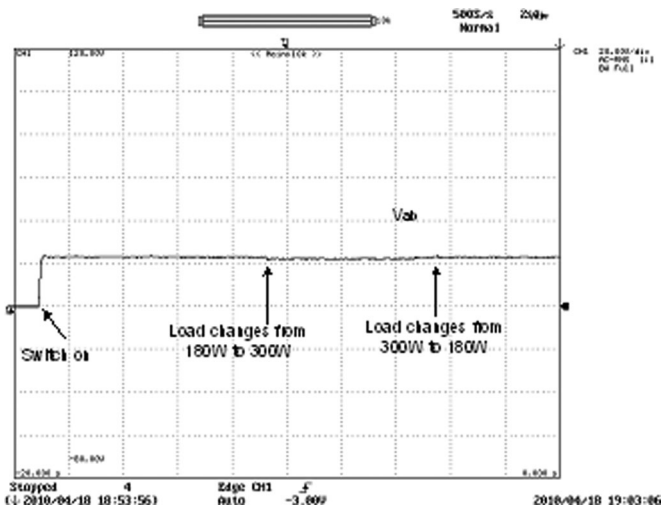

Fig. 25. Inverter terminal voltage (V_{ab}) for switch ON and step load changes.

The 230 V, 50 Hz line to neutral ac output voltage obtained at the secondary of delta/star step-up transformer is first scaled down to 3 V (up to the limits of DSP ADC) using ac voltage sensing cards. This analog voltage is converted into digital through ADC of the DSP controller and further scaled down to per unit value in scaling blocks. This per unit value is converted

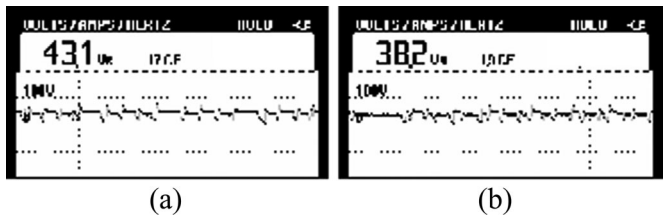

Fig. 26. Fuel-cell output for different loads. (a) 180 W (b) 300 W.

from *abc to dq*0 form and compared with the reference voltage signals *Vd*_ref *(= 1 pu)* and *Vq*_ref *(= 0)*. The deviation is processed through the PI controller to reduce the error signal.

The output of the PI controller is considered as modulation index *''m_a''* and is used to generate three modulating signals using *dq*0 *to abc* transformation. These signals are further scaled with the gain of half of the value of amplitude of carrier signal for the generation of pulses applied to the 3-phase MOSFET Bridge. Moreover, the externally generated ramp frequency signal *(sin_cos)* is used for the *abc to dqo* and *dqo to abc* conversion. Further, the switches of the inverters are controlled by comparing the output of sinusoidal *abc* waveform with the desired carrier signal. A graphical representation of PWM switch control is shown in Fig. 16. Here, the generated carrier waveform is compared with the reference modulating signal to generate the pulse pattern for three upper leg switches of inverter.

Usually, the ON state and OFF state of the power switches of inverter legs are always complimentary. The complementary signals are, therefore, generated internally in the DSP kit using logic states of NOT gate operation. This complete process of inverter control is performed by TMS320F2812 controller to regulate the fuel-cell characteristics.

VI. Experimental Results

To validate the performance of the proposed system, a laboratory proto-type of single stage power electronic interface is developed for the fuel-cell-based stand-alone applications as shown in Fig. 17. The system parameters are given in Table II.

The PWM control signals are generated using a low cost TMS320F2812 controller interfaced with MATLAB/Simulink in real time workshop. Fig. 18 shows the generated control pulses, which are applied to MOSFET switches after proper amplification and isolation using TLP250 IC.

The three-phase line to neutral output voltage waveform for 180 W resistance load is shown in Fig. 19. The inverter output voltage, load current, and frequency spectrum of 180 W resistive load are shown in Fig. 20(a) and (b), respectively. Fig. 21(a) and (b) shows the filtered output voltage at the primary side of transformer and its frequency spectrum. Fig. 22(a) and (b) shows the line to neutral ac output voltage and its frequency spectrum for a fixed modulation index of 0.57 at 180 W resistive load.

To validate the effectiveness of developed experimental setup, Fig. 23(a) and (b) shows filter output voltage and ac output voltage obtained through simulation for similar system parameters as given in Table II. It is observed that the filtered output voltage 7.10 V rms is lower than the inverter voltage 9.06 V rms due to the large drop in internal resistance of the filter components. However, the % THD at the inverter output voltage is reduced from 35.6% to 5% as shown in Fig. 20(b) and Fig. 21(b), respectively. As, the primary side input voltage is lower than the specified value, the line to neutral voltage at the load side is 117.1 V rms as shown in Fig. 22(a). The line to neutral ac output voltage can be set to 230 V rms by the increasing the value of modulation index. This can be observed from the closed loop control scheme developed in $dq0$ reference frame. Fig. 24(a) and (b) shows the frequency spectrum of inverter output voltage for load changes from 180 W to 300 W that is well regulated during the load increment by adjusting the modulation index. The transient response of inverter output voltage for varying loads is shown in Fig. 25. Moreover, it is observed from Fig. 26 that the drop in fuel-cell voltage is from 43.1 V to 38.2 V for corresponding load changes from 180 W to 300 W. This shows robustness of the developed controller for fuel cell based system.

VII. Conclusion

A laboratory proto-type of DSP-controlled power electronic interface for fuel-cell-based distributed generation has been developed. The complete description for generation of PWM control signals using TMS320F2812 DSP controller in real time workshop combined with MATLAB/Simulink model and CC-Studio is presented. The implemented DSP-based power electronic interface gives satisfactory performance for fuel-cell-based power electronic interface. The total harmonic distortion present at the inverter output is effectively reduced using a suitable LC filter. Experimental results prove the algorithm functionality and the validity of the developed setup. The experimental results obtained are validated through simulation for similar system parameters that illustrate the effectiveness of DSP-based control.

References

[1] R. Ramakumar and P. Chiradeja, "Distributed generation and renewable energy systems," in *Proc. 37th Intersoc. Energy Convers. Eng. Conf.,* IECEC-2002, Washington, DC, Jul. 2002, vol. 7, pp. 716–724.

[2] Z. Ye, M. Dame, and B. Kroposki, "Grid connected inverter anti islanding test results for general electric inverter based interconnection technology,", Nat. Renew. Energ. Lab., Boulevard, Golden, CO, Tech. Rep., NREL/TP-560-37200, Jan. 2005.

[3] R. A. Walling and N. W. Miller, "Distributed generation islanding – Implications on power system dynamic performance," in *Proc. IEEE Power Eng. Soc. Summer Meeting*, Chicago, Jul. 2002, vol. 1, pp. 92–96.

[4] Standards for Interconnecting Distributed Resources into Electric Power Systems, IEEE Standard 1547TM, Jun, 2003.

[5] List of Power outages. Available: http://en.wikipedia.org/wiki/List_of_power_outages

[6] H. Jiayi, J. Chuanwen, and X Rong, "A review on distributed energy resources and Microgrid," *Renewable and Sustainable Energy Rev.*, vol. 12, pp. 2472–2483, 2008.

[7] Y. W. Li and C. N. Kao, "An accurate power control strategy for power-electronics-interfaced distributed generation units operating in a low-voltage multibus microgrid," *IEEE Trans. Power Electron.*, vol. 24, no. 12, pp. 2977–2988, Dec. 2009.

[8] C. L. Chen, Y. Wang, J. S. Lai, Y. S. Lee, and D. Martin, "Design of parallel inverters for smooth mode transfer microgrid applications," *IEEE Trans. Power Electron.*, vol. 25, no. 1, pp. 6–15, Jan. 2010.

[9] R. Majumder, B. Chaudhuri, A. Ghosh, G. Ledwich, and F. Zare, "Improvement of stability and load sharing in an autonomous microgrid using supplementary droop control loop," *IEEE Trans. Power Syst.*, vol. 25, no. 2, pp. 796–808, May 2010.

[10] A. Payman, S. Pierfederici, and F. M. Tabar, "Energy management in a fuel cell/supercapacitor multisource/multiload electrical hybrid system," *IEEE Trans. Power Electron.*, vol. 12, no. 12, pp. 2681–2691, Dec. 2009.

[11] M. Din, M. N. Marwali, J. W. Jung, and A. Keyhani, "Power flow control of a single distributed generation unit," *IEEE Trans. Power Electron.*, vol. 23, no. 1, pp. 343–352, Jan. 2008.

[12] H. Kakigano, Y. Miura, and T Ise, "Low voltage bipolar type DC microgrid for super high quality distribution," *IEEE Trans. Power Electron.*, vol. 25, no. 12, pp. 3066–3075, Dec. 2010.

[13] A. Kirubakaran, R. K. Nema, and S. Jain, "Distributed generation by solid oxide fuel cell: A review," in *Proc. Power Syst. Technol. and IEEE Power India Conf.*, Oct. 2008, pp. 1–6.

[14] A. B. Stambouli and E. Traversa, "Fuel cells, an alternative to standard sources of energy," *J. Renew. Sust. Energ. Rev.*, vol. 6, pp. 297–306, 2002.

[15] X. Huang, Z. Zhang, and J. Jiang, "Fuel cell technology for distributed generation: An overview," in *Proc. IEEE Symp. Ind. Electron*, Montreal, Que, Jul. 2006, pp. 1613–1618.

[16] S. Pasricha, M. Keppler, S. R. Shaw, and M. H. Nehrir, "Comparison and identification of static electrical terminal fuel cell models," *IEEE Trans. Energy Convers.*, vol. 22, no. 3, pp. 746–754, Sep. 2007.

[17] A. Kirubakaran, S. Jain, and R. K. Nema, "A review on fuel cell technologies and power electronic interface," *J. Renew. Sust. Energ. Rev.*, vol. 3, pp. 2430–2440, Dec. 2009.

[18] W. Choi, P. N. Enjeti, and J. W. Howze, "Development of an equivalent circuit model of a fuel cell to evaluate the effects of inverter ripple current," in *Proc. IEEE Appl. Power Electron. Conf. Expo.*, Feb. 2004, pp. 355–361.

[19] S. K. Mazumder, R.K. Burra, R. Huang, M. Tahir, and K. Acharya, "A universal grid-connected fuel cell inverter for residential application," *IEEE Trans. Ind. Electron.*, vol. 57, no. 10, pp. 3431–3447, Oct. 2010.

[20] K. Chaniago, J. Selvaraj, and N. A. Rahim, "Implementation of single-phase grid connected inverter using TMS320F2812," in *Proc. 3rd IEEE Conf. Ind. Electron. Appl.*, Singapore, Jun. 2008, pp. 1498–1502.

[21] M. A. A. Younis, N. A. Rahim, and S. Mekhilef, "Distributed generation with parallel connected inverter," in *Proc. 4th IEEE Conf. Ind. Electron. Appl.*, Xi'an, China, May, 2009, pp. 2935–2940.

[22] W. Zhang, G. Feng, Y. F. Liu, and B. Wu, "A digital power factor correction (PFC) control strategy optimized for DSP," *IEEE Trans. Power Electron.*, vol. 19, no. 6, pp. 1474–1485, Nov. 2004.

[23] L. J. Xue and J. Liu, "Simulation and experiment of induction motor controller," in *Proc. Int. Conf. Comput. Autom. Eng.*, Bangkok, Thailand, 2009, pp. 54–58.

[24] L. O. Pop, L. G. Chindris, and S. A. Dulf, "Using DSP technology for true sine PWM generators for power inverters," in *Proc. 27th Int. Spring Seminar on Electron. Technol.*, Bankya, Bulgaria, May 2004, pp. 141–146.

[25] W. Li, G. Xu, H. Tong, and Y. Xu, "Design of vehicle control unit based on DSP for a parallel HEV," in *Proc. IEEE Int. Conf. Autom. Logistics*, Aug. 2007, pp. 1597–1601.

[26] D. Hercog, M. Curkovic, and K. Jezernik, "DSP based rapid control prototyping systems for engineering education and research," *IEEE Proc. Conf. Comput. Aided Control Syst. Design*, pp. 2292–2297, Oct. 2006.

[27] M. U. Cuma, A. Teke, M. Tumay, K. C. Bayindir, and M. S. Ozgur, "Experimental architecture of a DSP based signal generation for PWM inverter," *J. Comput. Appl. Eng. Education*, pp. 1–13, 2009.
[28] F. Blaabjerg, Z. Chen, and S. B. Kjaer, "Power electronics as efficient interface in dispersed power generation systems," *IEEE Trans. Power Electron.*, vol. 19, no. 5, pp. 1184–1194, Sep. 2004.
[29] J. Anziceek and M. Thompson, "DC-DC boost converter design for kettering university's GEM fuel cell vehicle," in *Proc. Electr. Insul. Conf. Electr. Manuf. Expo.*, Indianapolis, Oct. 2005, pp. 307–316.
[30] X. Kong, L. Thian Choi, and M. K. Ashwin, "Analysis and control of isolated current-fed full bridge converter in fuel cell system," in *Proc. 30th Annu. Conf. IEEE Ind. Electron. Soc.*, Busan, South Korea, Nov. 2004, pp. 2825–2830.
[31] T. A. Nergaard, J. F. Ferrell, L. G. Leslie, and J. S. Lai, "Design considerations for a 48V fuel cell to split single phase inverter system with ultra capacitor energy storage," in *Proc. Power Electron. Spec. Conf.*, Australia, 2002, pp. 2007–2012.
[32] J. Wang, F. Z. Peng, J. Anderson, A. Joseph, and R. Buffenbarger, "Low cost fuel cell converter system for residential power generation," *IEEE Trans. Power Electron.*, vol. 19, no. 5, pp. 1315–1322, Sep. 2004.
[33] G. K. Anderson, C. Klumpner, S. B. Kjter, and F. Blaabjerg, "A green power inverter for fuel cells," in *Proc. Power Electron. Spec. Conf.*, Australia, 2002, vol. 2, pp. 727–733.
[34] A. M. Tuckey and J. N. Krase, "A low cost inverter for domestic applications," in *33rd Annu. IEEE Power Electron. Spec. Conf.*, Australia, 2002, pp. 339–346.
[35] J. Mazumdar, I. Batarseh, N. Kutkut, and O. Demirci, "High frequency low cost DC-AC inverter design with fuel cell source for home applications," *Proc. 37th IAS Annu. Meet. Ind. Appl. Conf.*, Pennsylvania, USA, vol. 2, 2002, pp. 789–794.
[36] R. Gopinath, S. Kim, J. H. Hahn, P. N. Enjeti, M. B. Yeary, and J. W. Howze, "Development of a low cost fuel cell inverter system with DSP control," *IEEE Trans. Power Electron.*, vol. 19, no. 5, pp. 1256–1262, Sep. 2004.
[37] S. Jung, Y. Bae, S. Choi, and H. Kim, "A low cost utility interactive inverter for residential fuel cell generation," *IEEE Trans. Power Electron.*, vol. 22, no. 6, pp. 2293–2298, Nov. 2007.
[38] S. J. Jang, C. Y. Won, B. K. Lee, and J. Hur, "Fuel cell generation system with a new active clamping current-fed half-bridge converter," *IEEE Trans. Energy Convers.*, vol. 22, no. 2, pp. 332–340, Jun. 2007.
[39] Z. B. Shen and E. L. El-Saadany, "Novel interfacing for fuel cell based distributed generation," *IEEE Power Eng. Soc. Gen. meet.*, Tampa, FL, Jun. 2007, pp. 1–6.
[40] L. Zubiet and G. Panza, "A wide input voltage and high efficiency DC-DC converter for fuel cell applications," in *Proc. 20th Annu. IEEE Appl. Power Electron. Conf. Expo.*, vol. 1, Texas, 6-10, Mar. 2005, pp. 85–89.
[41] H. Xu, X. Wen, and L. Kong, "High power DC-DC converter and fuel cell distributed generation system," in *Proc. 39th IAS Annu. Meet. Record IEEE ind. Appl. Conf.*, Seattle, Oct. 2004, vol. 2, pp. 1134–1139.
[42] J. S. Lai, "A high performance V6 converter for fuel cell power conditioning system," *in Proc. IEEE Conf. Vehicle Power & Propulsion*, Sep. Chicago, 2005, pp. 624–630.
[43] Y. J. Song, S. K. Chung, and P. N. Enjeti, "A current-fed HF link direct DC/AC converter with active harmonic filter for fuel cell power systems," in *Proc. 39th IAS Annu. Meet. IEEE Ind. Appl. Conf.*, Seattle, Oct. 2004, pp. 124–128.
[44] C. Liu, A. Johnson, and J.S. Lai, "Modeling and control of a noval six-leg three phase high –power converter for low voltage fuel cell applications," *IEEE Trans. Power Electron.*, vol. 21, pp. 1292–1300, 2006.
[45] Y. H. Kim, H. W. Moon, S. H. Kim, E.-J. Cheong, and C.-Y. Won, "A fuel cell system with Z source inverters and ultra capacitors," in *Proc.4th Int. Power Electron. Motion Control Conf.*, Xi'an, Lorea, Aug. 2004, pp. 1587–1591.
[46] R. J. Wai, R. Y. Duan, J. D. Lee, and L. W. Liu, "High efficiency fuel cell power inverter with soft switching resonant technique," *IEEE Trans. Energy Convers.*, vol. 20, no. 2, pp. 485–492, Jun. 2005.
[47] K. Jin, X. Ruan, M. Yang, and M. Xu, "Power management for fuel cell power system cold start," *IEEE Trans. Power Electron.*, vol. 24, no. 10, pp. 2391–2395, Oct. 2009.
[48] S. Jain, J. Jiang, X. Huhang, and S. Stvandic, "Single stage power electronic interface for a fuel cell based power supply system," in *Proc. IEEE Electr. Power Conf.*, Canada, Oct., 2007, pp. 201–206.
[49] M. Tanrioven and M. S. Alam, "Modeling, control, and power quality evaluation of PEM fuel cell-based power supply system for residential use," *IEEE Trans. Ind. Appl.*, vol. 42, no. 6, pp. 1582–1589, Nov./Dec. 2006.
[50] N. Mohan, T. M. Undeland, and W. P. Robbins, *Power Electronics Converters, Applications and Design*, 3rd ed. Hoboken, NJ: Jon Wiley & Sons, 2001.
[51] Y. H. Li, S. S. Choi, and S. Rajakaruna, "The design of the inverter output filter of a fuel cell power plant in an isolated system," in *Proc. 5th Int. Conf. Power Electron. Drives Syst.*, Singapore, Nov. 2003, vol. 1, pp. 548–553.
[52] S. Jain, J. Jiang, X. Huhang, and S. Stvandic, "Modeling of fuel cell based power supply system for grid interface," in *Proc. IEEE Powercon 2008*. New Delhi, Oct. 2008, pp. 1–8.
[53] A. H. Niasar, H. Moghbeli, and A. Vahedi, "Implementation of four switch brushless DC motor drive based on TMS320F2407A DSP," in *Proc. IEEE Int. Conf. Signal Process. Commun.* Dubai, Nov. 2007, pp. 332–335.
[54] Mathworks Embedded C2000 Target, (Jan 2004). [Online]. Available: http://www.mathworks.com/products/rtw/
[55] Texas Instruments Inc. *TMS320×281x DSP Analog-to-Digital Converter (ADC) Reference Guide* Houston, TX: Texas Instruments Inc., 2004.
[56] Texas Instruments, *Code Composer Studio™ IDE*. Houston, TX: Texas Instruments Inc., 2009. Available: http://www.ti.com.
[57] Texas Instruments, "C2812 Design Workshop" Students Manual", May 2004. http://www.ti.com.
[58] N. Bulic, M. Miletic, and I. Erceg, "DSP based system for synchronous generator excitation control," in *Proc. Electr. Drives and Power Electron.*. Dubrovnik, Croatia, EDPE 2005, pp. 1–5.
[59] Texas Instruments, "TMS32081xDSP Event Manager (EV) Reference Guide," Jun. 2007. Available: focus.ti.com/lit/ug/spru065e/spru065e.pdf.
[60] A. Y. E. Lesan, M. L. Doumbia, and P. Sicard, "DSP-based sinusoidal PWM signal generation algorithm for three phase inverters," in *Proc. IEEE Electr. Power & Energy Conf.*, 2009, pp. 1–6.

Annamalai Kirubakaran received the B.E degree in electrical and electronics engineering from Madras University, India, and M.E degree in power system from Annamalai University, India, in 2002 and 2004, respectively, and the Ph.D. degree in electrical engineering from Maulana Azad National Institute of Technology, Bhopal, India, in 2011.

Currently, he is an Associate Professor at the School of Electrical Engineering, VIT University, Vellore, India. His research interests include fuel-cell-based distributed generation, energy storage devices, and their applications to power system.

Shailendra Jain received the B.E.(elect.), M.E.(power elex), and Ph.D. degrees, in 1990, 1994, and 2003, respectively.

He is currently working as an Associate Professor in the Department of Electrical Engineering, Maulana Azad National Institute of Technology, Bhopal, India. He has been awarded "Career Award for Young Teachers" by All India Council for Technical Education (AICTE) New Delhi, India, for the year 2003-2004. He received a postdoctoral fellowship at the University of Western Ontario (UWO) London, ON, Canada, in 2007. His research interests include power electronics and electric drives, power quality improvement, active power filters, high-power factor converters, and fuel-cell-based distributed generation.

Rajesh Kumar Nema received the Ph.D. degree in electrical engineering from Barkatullah University, Bhopal, India, in 2004.

He is currently an Associate Professor in the Department of Electrical Engineering, Maulana Azad National Institute of Technology, Bhopal, India. His current research interests include power conditioning unit for renewable energy storage system particularly solar energy, hybrid energy systems, and grid interconnection of renewable energy sources.